JOURNAL OF CATALYSIS 134, 1–12 (1992)

Reactivity of CO on Vanadium-Promoted Rhodium Catalysts as Studied with Transient Techniques

TIJS KOERTS, WIM J. J. WELTERS, AND RUTGER A. VAN SANTEN

Schuit Institute of Catalysis, Department of Inorganic Chemistry and Catalysis, Eindhoven University of Technology, PO Box 513, 5600 MB Eindhoven, The Netherlands

Received March 4, 1991; revised July 22, 1991

The effect of vanadium promotion on the kinetics of CO methanation on silica-based rhodium catalysts was probed. Transient model experiments employing temperature-programmed surface reaction spectroscopy and pulse surface reaction rate analysis were used to unravel changes in rates of elementary reaction steps. CO dissociation is the rate-limiting step in the overall methanation reaction. The rate of CO dissociation is found to be enhanced by vanadium. The activation energy is lowered from 90 kJ/mol for Rh/SiO_2 to 65 kJ/mol for the promoted catalyst. The activation energy for CO dissociation is not dependent on the hydrogen partial pressure, while it is a strong function of the CO surface coverage. CO adsorption at temperatures above 250°C results in very reactive surface carbonaceous intermediates. Even at −15°C methane formation was observed upon hydrogenation. This reactive surface carbon can be incorporated in higher hydrocarbons. This process is favoured by vanadium promotion.

INTRODUCTION

It is well established that on rhodium catalysts synthesis gas can be converted into oxygenates (*1, 2*). Oxides of transition metals such as TiO_2, V_2O_3, ThO_2, Fe_2O_3, La_2O_3, ZrO_2, and Mo_2O_3 can shift the product selectivity to methane, higher hydrocarbons, methanol, or higher oxygenates formation (*3–9*). Vanadium-promoted rhodium catalysts have been reported to have a high selectivity at low conversion for the production of ethanol (*10, 11*). An important observation was the significantly enhanced activity of such promotion (*10*). The mechanism for the formation of C_2 oxygenates as well as hydrocarbons has been extensively studied. A common elementary reaction step in the route towards hydrocarbons and higher oxygenates is the dissociation of an adsorbed CO molecule into adsorbed carbon and oxygen atoms.

Because CO dissociation is a difficult step on rhodium, its rate controls the activity for the synthesis gas reaction. With various surface science techniques CO dissociation has been studied on single crystals showing that CO dissociation is impossible or very slow on flat surfaces such as f.c.c. Rh (111) (*12, 13*). The introduction of steps and kinks can enhance the rate of CO dissociation (*13, 14*). Small metal particles supported on silica allow CO dissociation at temperatures above 250°C, as first detected by Solymosi and Erdöhelyi (*15*). Many articles have dealt with the influence of the support on CO dissociation in relation to catalytic activity in synthesis gas conversion (*16–19*). Ichikawa *et al.* (*20*) proposed that the influence of the carrier is related to its acid/basic properties. Furthermore, the metal particle size can be a factor of importance for CO dissociation. Sachtler and Ichikawa (*6*) showed that blocking atoms on Group VIII metals are able to decrease the rate for CO dissociation, which is a structure-sensitive reaction. CO dissociation needs a metal ensemble of at least five to seven free metal surface atoms (*21*), as indicated with quantum chemical calculations. This implies that metal particles of a size below 15 Å will show decreased CO dissociation activity. Moreover, it has been proposed from infrared measurements (*22*) that bridge-adsorbed

0021-9517/92 $3.00

CO is the favoured configuration for CO dissociation on supported rhodium catalysts.

Sachtler *et al.* (*23*) suggested a mechanism explaining the promotion of CO dissociation by oxidised transition metals. Chemisorbed CO is activated through an interaction of its oxygen end bending to an oxophilic promoter. Using infrared spectroscopy others (*24–26*) have suggested the observation of such "tilted" adsorbed CO. Ichikawa *et al.* (*27, 28*) suggested that multivalent reduced transition metals are able to dissociate CO in a redox mechanism. Reduced transition-metal M^{n+} ions can be oxidised to $M^{(n+2)+}$ by oxygen supplied by dissociated CO. Subsequent reduction occurs by CO or H_2 to again form M^{n+}.

Here we study the kinetics of CO dissociation on supported rhodium catalysts with model experiments of temperature-programmed surface reaction spectroscopy (TPSR) (*29–31*) and pulse surface reaction rate analysis (PSRA) (*32*). TPSR can be used to titrate different surface species from a metal surface quantitatively. Also different active sites can be distinguished according to their reactivity. It is possible to determine the activation energy for methanation from a well-defined TPSR plot. Using this, the influence of the hydrogen pressure and CO coverage on the activation energy for CO dissociation is studied. The influence of vanadium promotion on CO dissociation will also be analysed with these two non-steady-state techniques of PSRA and TPSR.

By adsorbing CO dissociatively at elevated temperatures carbonaceous intermediates can be generated. The reactive carbidic surface species on the rhodium and rhodium–vanadium catalysts are compared with respect to their reactivity for carbon–carbon bond formation in synthesis gas.

EXPERIMENTAL

Catalyst

A 3 wt% rhodium catalyst was prepared by incipient wetness impregnation of an aqueous solution of $RhCl_3$ on preshaped Grace 332 type silica, mesh size 75–125, 300 m^2/g. After impregnation, the catalyst was dried overnight at 110°C. The catalyst was reduced for 24 h at 350°C in a flow of 30% H_2 in N_2. The temperature was raised 2°C/min. After cooling to room temperature the catalyst was passivated by pulsing oxygen in the nitrogen flow. To compare Rh and RhV catalysts with the same particle size vanadium was added by post-impregnation from a solution of NH_4VO_3 in water. The ratio Rh/V was 3 on a molar basis. The catalyst was again dried at 110°C. The low amount of added vanadium resulted in a catalyst system in which the CO chemisorption capacity is hardly influenced by the reduction temperature.

Another 4.7 wt% rhodium catalyst was prepared by wet impregnation of $RhCl_3$ on Aerosil 200 type silica (200 m^2/g). After reducing and passivating, vanadium was added to this system by wet post-impregnation with a solution of $VOCl_2$ in a mixture of 50% ethanol and 50% 5 *M* HCl (Rh/V = 2 on a molar basis). For both catalyst systems the amount of added vanadium was chosen in such a way that the CO chemisorption capacity was reduced by about 50%.

Method

For each experiment 300 mg of the catalyst was placed in the reactor tube (i.d. = 10 mm) and was reduced *in situ* between 300 and 450°C in a flow of about 8% hydrogen in helium. At the first reduction the temperature was raised not faster than 5°C/min. This prevented the catalyst from sintering. The experiments were performed in a reactor flow system (see Fig. 1). The reaction gases were analysed on line by a quandrupole mass spectrometer (type: pga 100 from Leybold).

All gases were oxygen purified with a BTS column (reduced copper). Water was extracted from the gases using a molecular sieve. An extra molecular sieve column was added for the hydrogen and helium gases,

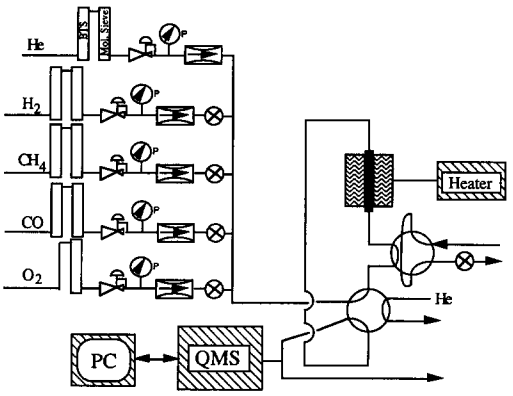

FIG. 1. Schematic representation of the pulse reactor flow system with on-line detection with a quadrupole mass spectrometer.

which could be cooled at liquid nitrogen temperature to reduce the water concentration below parts per million level. In all cases the carrier gas was helium.

CO chemisorption was performed from a flow of 55 ml/min of 0.5% CO in He at 1 atmosphere. From the consumed amount of CO the catalyst metal dispersion could be calculated.

Temperature-programmed surface reaction spectroscopy experiments were performed after the creation of surface species from CO. The flow was 20 ml/min of 7.5% hydrogen in helium while the temperature was raised with 5 or 10°C/min. The formation of methane, water, and carbon dioxide, as well as CO desorption, could be monitored on line in one experiment as a function of the temperature.

During pulse surface reaction rate analysis experiments a volume of 0.19 ml of 3 atm of 5% CO in He was pulsed into a flow of 50 ml/min 3% hydrogen in helium. At a fixed temperature the reactivity of pulsed CO to methane was measured.

Unless stated otherwise, the experiments were performed with the catalyst systems prepared on Grace-type silica. These catalysts had a higher dispersion and their preparation was more reproducible and consisted of a well-defined mesh size.

Characterization

The rhodium particle size of the unpromoted catalysts was determined by transmission electron microscopy (TEM) as well as by CO chemisorption (see Table 1). The rhodium particle size in the rhodium/vanadium systems could only be determined from TEM because vanadium coadsorption reduces the amount of CO chemisorption (*33*).

The particle size as determined by TEM is in good agreement with that obtained with chemisorption for the unpromoted rhodium catalysts on Grace silica. The rhodium particle size measured by TEM was the same with or without vanadium on the Grace silica-supported catalyst (in contrast with CO chemisorption, where CO/Rh = 0.55 and 0.22, respectively).

On the RhV catalyst supported on Grace-type silica, small amounts of vanadium were not in contact with the rhodium, as could be observed with TEM. This was also suggested from temperature-programmed reduction (TPR) (Fig. 2) measurements.

Most of the vanadium reduces at the same temperature as the rhodium, suggesting a very good interaction between the vanadium and the rhodium metal particles. This result is in good agreement with Kip *et al.* (*34*) and Bastein (*31*) who measured TPR spectra as a function of the vanadium con-

TABLE 1

Results of CO Chemisorption and TEM

Catalyst	Carrier	CO/Rh[a] (Å)[b]	Rh Particle Size (Å)[c]
3% Rh	Grace 332	0.55 (20)	22
Rh/V = 3	Grace 332	0.26 (53)	22
4.7% Rh	Aerosil 200	0.30 (45)	35
Rh/V = 2	Aerosil 200	0.12 (125)	50

[a] Mol CO chemisorbed per mol rhodium.

[b] Calculated particle size from CO chemisorption using a pyramid model assuming that every surface rhodium atom adsorbs one CO molecule.

[c] From TEM measurements.

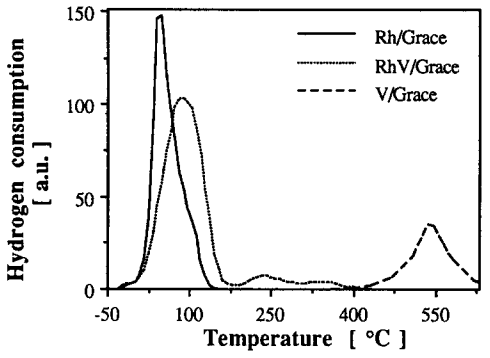

FIG. 2. Temperature-programmed reduction of Rh/Grace silica (solid line), RhV/Grace silica (dotted line), and V/Grace silica (dashed line). The temperature was raised at 7.8°C/min in a flow of 4% hydrogen in argon. Before TPR the catalysts were calcined at 350°C.

TABLE 2

Activity and Selectivity during Synthesis Gas Reaction at 200°C

Catalyst	Rh/Grace	RhV/Grace	Rh/Aer.[c]	RhV/Aer.[c]
CO Conversion (%)	0.21	0.80	0.22	0.85
Activity[a]	0.18	0.70	0.15	0.52
Methane selectivity (%)[b]	28	24	50	23
C_2^+ hydrocarbon sel.[b]	18	22	16	21
Ethanol selectivity[b]	32	36	7.1	39
Ethanal selectivity[b]	12	4.2	22	5.1
Other oxo's selectivity[b]	10	13.8	4.8	12

[a] Activity in mmol CO converted per mol surface Rh per second.
[b] Selectivities expressed in carbon efficiency.
[c] Aer., Aerosil 200-type silica.

tent in, respectively, $Rh_2O_3/V_2O_5/Al_2O_3$ and $Rh_2O_3/V_2O_5/SiO_2$ catalysts. Some of the vanadium, about 15%, reduces at higher temperature, between 160 and 400°C. This second peak may be due to vanadium, which has no interaction with the rhodium metal particles, although the reduction temperature of vanadium on Grace silica is higher, around 500°C. The difference in reduction temperature may be induced by the smaller more defect-rich vanadium particles, which reduce at lower temperature (*36*). Also spillover hydrogen, dissociated by the rhodium particles, can be the reason of the lower reduction temperature of the vanadium particles.

The rhodium metal particles reduce at a higher temperature in the vanadium-promoted system, which also indicates their close contact with the promoter.

An interesting surface morphology characterization probe is the hydrogenolysis of ethylene to methane. Carbon–carbon bond cleavage is known to be a structure-sensitive reaction (*37, 38*). Larger metal ensembles are needed for the formation of methane from ethylene and hydrogen. Figure 3 shows the activity for the rhodium and rhodium–vanadium catalyst for this reaction.

The rate of the hydrogenolysis reaction is obviously reduced by the vanadium promoter, suggesting a decrease in metal atom ensemble size. It confirms the presence of the vanadium promoter adsorbed on the surface of the rhodium metal particles. Apparently vanadium oxide precipitates preferentially on the rhodium metal particles during post-impregnation.

Finally, the catalysts were characterised by their catalytic performance with respect to the synthesis-gas conversion reaction. Activity and selectivity were measured under differential conditions (conversion <1%), after 1 h of steady-state reaction at 200°C in a flow of 15 ml/min ($H_2/CO = 2$). The results are presented in Table 2.

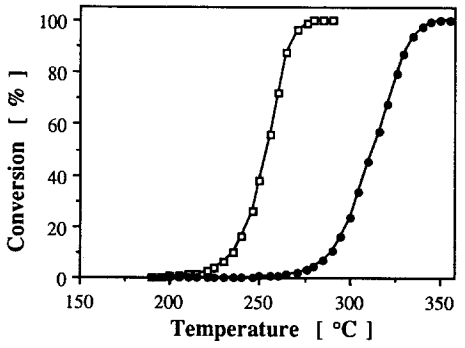

FIG. 3. Hydrogenolysis of ethylene on Rh/Grace silica (squares) and RhV/Grace silica (circles) catalyst in a flow of 56 ml/min of 9% hydrogen and 1.6% ethylene in helium, as a function of the temperature.

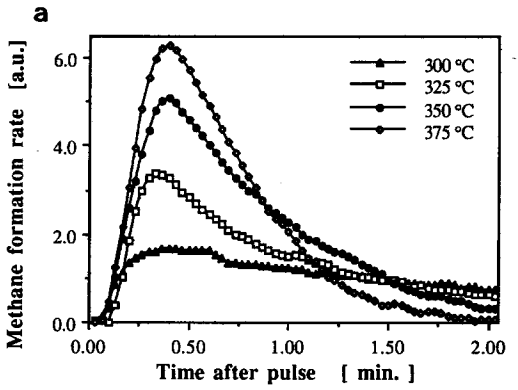

FIG. 4a. Methane formation from a short CO pulse in a diluted hydrogen flow over Rh/Aerosil catalyst at different temperatures.

The differences in selectivities between the Grace 332 and Aerosil 200-type silica for the unpromoted catalysts have been noted by Nonneman *et al.* (*39, 40*) who ascribed this to impurities in the silica. The Grace 332 carrier contains, in addition to silica, Na 0.04%, CaO < 0.005%, and Fe_2O_3 < 0.01%. The catalytic activity is increased by about a factor of 4 through vanadium promotion on both types of silica support.

RESULTS AND DISCUSSION

The rates of methane formation as determined by PSRA as a function of the temperature are presented in Fig. 4a. During PSRA experiments the following processes take place: CO adsorption, subsequent CO dissociation, and hydrogenation of surface intermediates. CO adsorption on the clean reduced metal particles is very fast and not activated. On rhodium catalysts CO dissociation is the rate-determining step for methane formation. This was concluded by Mori *et al.* (*32*) from PSRA data. They showed that the rate of CO dissociation, k_{CO}, is much smaller than K_{CH_x}, the rate of surface CH_x hydrogenation. Therefore one can calculate turnover frequencies for CO dissociation from PSRA curves.

The methane formation rate is considered to be first order in adsorbed CO, which is normal for adsorbed surface species. The integrated methane formation rate as a function of time can therefore be written according to Eq. (1), in which k is the turnover frequency per second for CO dissociation.

$$r_{CH_4}(t) = P_{H_2}^{\beta}\theta_{CO_{t=0}}ke^{-kt}. \qquad (1)$$

The value of β lies between 1 and 2 and is not important to the fit as long as it does not change during the reaction. From the curve of $\ln(r_{CH_4})$ against time t, the reactivity constant k is obtained from the slope. However, this line is only straight in the decreasing part of the curve (for the fit the data points are taken in the decreasing part after 75% of the maximum height is achieved).

Also the whole PSRA curves can be fitted taking the nonideal performance of the reactor system into account. Equation (2) describes the methane formation curves in which the reactor is considered as one continuously stirred tank reactor.

$$r_{CH_4}(t) = A[e^{-kt} - e^{-t/\tau}]. \qquad (2)$$

Factor A is a preexponential and is a function of k, $P_{H_2}^{\beta}\theta_{CO_{t=0}}$, and τ. The mean resi-

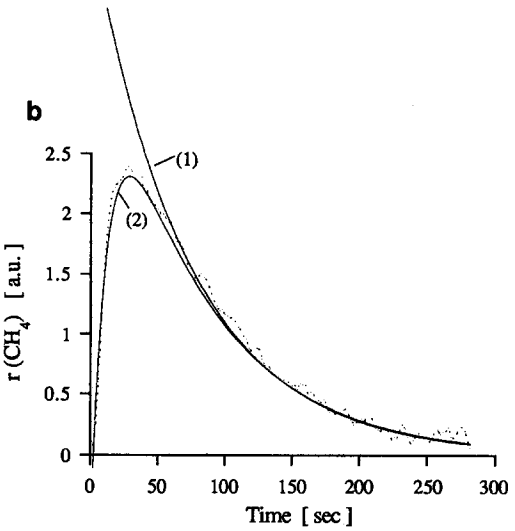

FIG. 4b. Different fit procedures for a PSRA curve. Dotted line: PSRA data at 350°C on a rhodium catalyst. Line (1), exponential fit according to Eq. (1); line (2), fit according to Eq. 2.

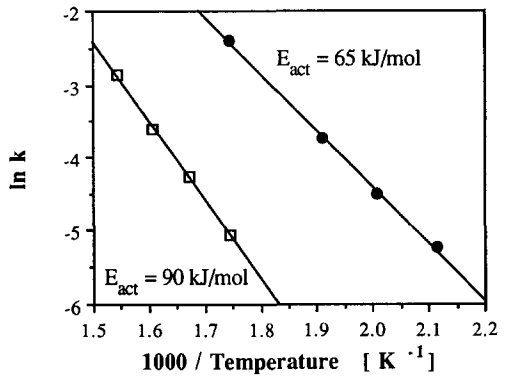

FIG. 5. Arrhenius plot from PSRA data for CO dissociation on Rh/Aerosil 200 (squares) and Rh,V/Aerosil 200 (circles). k values are expressed in turnover frequency (s^{-1}).

dence time in the reactor τ can be measured in a separate experiment in which a CO pulse is given over a silica catalyst bed; τ appeared to be 5 s. The results of both fit procedures are shown in Fig. 4b.

The fitted k values as found with the two procedures differ by only 2%, indicating that the reactor does not disturb the transient response at response times above 50 s. The values of the reaction rate constants as deduced with Eq. (1) for the Rh and RhV catalyst systems are shown, as a function of the temperature, in the Arrhenius plot of Fig. 5. It is clear that the CO dissociation rate is greatly enhanced by vanadium promotion. The activation energy for CO dissociation is lowered from 90 to 65 kJ/mol by vanadium. This agrees well with the results obtained by Mori and co-workers (*7, 32, 41, 42*). They noted that vanadium promotion on a ruthenium catalyst decreased the activation energy for CO dissociation (*7, 39*).

The affinity of adsorbed CO for dissociation can also be studied with TPSR. The rate of methanation of adsorbed CO as a function of temperature is described by the profiles of Fig. 6. During the hydrogenation of adsorbed CO, methane and water are the only products. The formation of water as a function of the temperature is the same as that for methane formation. This indicates that water and methane formation have the same rate-limiting step when CO is hydrogenated. This was also concluded for nickel by McCarty and Wise (*30*). The total area below the RhV curves is less than that under the unpromoted catalyst because the CO chemisorption capacity is reduced by the vanadium. Characteristic in these plots is the lower temperature for the maximum methane formation rate of the vanadium-promoted catalyst (*31*). Notwithstanding the lower number of adsorbed CO molecules on the RhV system, the reaction rate of methane formation is higher at low temperatures. The TPSR curves can be described with equation 3 (*43, 44*):

$$r_{CH_4(T,\theta_{CO})} = \nu_{eff(\theta_{CO})}\theta_{CO}e^{-E_a/RT} \qquad (3)$$

When θ_{CO} is taken constant in a very small temperature range in the beginning of the curve, it is possible to convert these data into an Arrhenius plot and derive an activation energy (Fig. 7). It appears that the CO methanation activity is increased by vanadium promotion, decreasing the activation energy from 96 to 67 kJ/mol, which is in good agreement with the activation energy derived from PSRA data. This confirms that CO dissociation is rate limiting. Although the rhodium surface metal ensembles are decreased by vanadium promotion, as shown with hydrogenolysis, the rate of CO dissociation is increased.

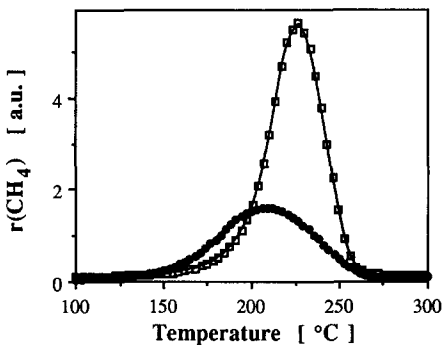

FIG. 6. Temperature-programmed hydrogenation of adsorbed CO on the Rh/Grace silica (squares) and the RhV/Grace silica (circles) catalysts.

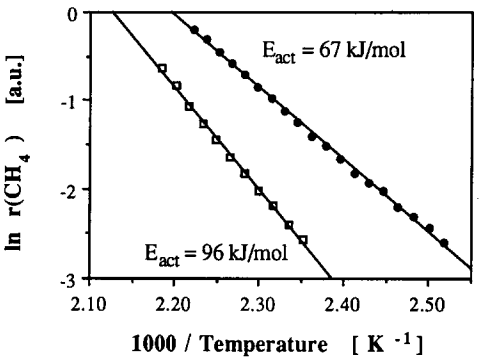

FIG. 7. Arrhenius plot from TPSR data for the Rh/Grace silica (squares) and the Rh,V/Grace silica (circles) catalyst.

With TPSR the activation energy for CO dissociation can be determined under well-defined conditions. The activation energy for this step was studied as a function of the surface coverage of CO. Homogeneous CO surface coverages on a rhodium catalyst were created by adsorbing a monolayer of CO and the subsequent removal of a known part by hydrogenation.

The TPSR curves of Fig. 8a show that under 200°C the methanation rate can be increased by decreasing the surface coverage of CO from 1 to 0.5. Also the temperature at which methane formation is maximal decreases when θ_{CO} decreases, indicating that CO dissociation is easier at low CO coverages. Figure 8b shows the Arrhenius plots from TPSR data as a function of the initial surface coverages of CO using Eq. (3).

The activation energy for CO dissociation is clearly a function of the surface coverage of CO. At low surface coverage the measured activation energy is 45 kJ/mol while it increases to about 90 kJ/mol at a CO coverage of a monolayer. This result is in agreement with findings of Marbrow and Lambert (*45*). They noted that CO dissociation is slower at higher CO pressures.

Apparently the overall effect of V_2O_3 coadsorption on the rate of CO dissociation is very similar to the effect of a decrease of CO coverage. In both cases the activation energy for CO dissociation is found to be decreased. Therefore we suggest another way to promote CO dissociation: CO dissociation is enhanced by making oxygen vacancies more available, because CO dissociation needs vacancies. We suggest that V^{3+} generates additional sites. Reduced vanadium can possibly supply oxygen vacancies, which enhances CO dissociation. In this way vanadium would act as a structural pro-

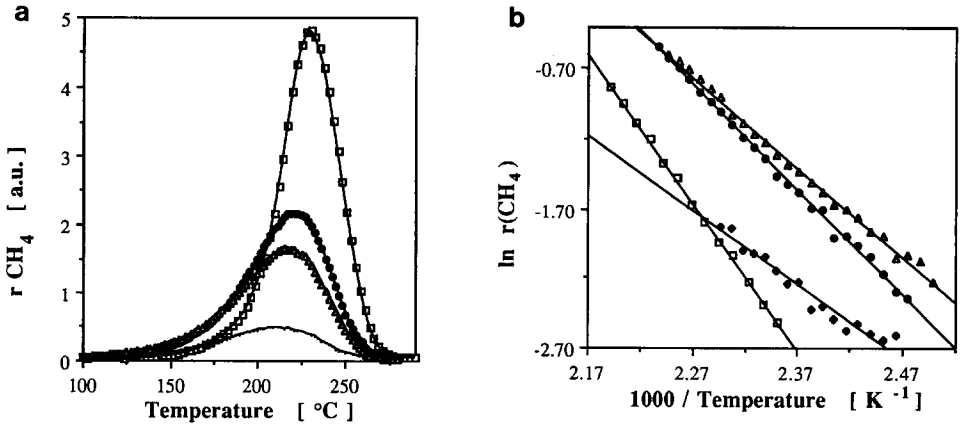

FIG. 8. TPSR curves obtained with different initial surface coverages of CO. (a) TPSR curves: squares, θ_{CO} = 1.00; circles, θ_{CO} = 0.65; triangles, θ_{CO} = 0.15; line, θ_{CO} = 0.15. (b) Arrhenius plot: squares, θ_{CO} = 1.00; circles, θ_{CO} = 0.65; triangles, θ_{CO} = 0.15; diamonds, θ_{CO} = 0.15.

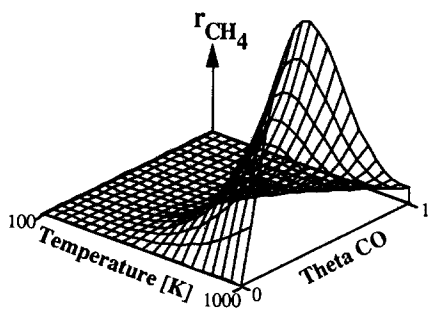

FIG. 9. Calculated methanation activity of adsorbed CO on the rhodium catalyst as a function of surface coverage and temperature according to Eqs. (3) and (4).

moter. This supports the hypothesis of Ichikawa that V_2O_3 can interact with adsorbed CO through an interaction with the oxygen end of CO, enhancing CO dissociation.

The function that describes the dependence of the activation from the CO surface coverage can be estimated from Fig. 9. A second-order approximation of the activation energy as a function of the CO coverage is given in

$$E_{act}(\theta_{CO}) = 43.64 - 1.48\,\theta_{CO} + 46\,\theta_{CO}^2\,(\text{kJ/mol}). \quad (4)$$

Knowing the activation energy as a function of the surface coverage Eqs. (3) and (4) can be used to calculate the rate for CO dissociation at any temperature and CO coverage (Fig. 9). This figure shows that there is an optimum CO surface coverage for methanation at a specified temperature. The CO surface coverage, at which CO dissociation activity is highest, is 0.2 at 100 K and increases slightly at higher temperatures to 0.33 at 1000 K. In creating rhodium catalysts with optimum methanation performance one should try to obtain this value.

The influence of the hydrogen partial pressure on the activation energy for CO dissociation was studied using TPSR and is shown in the Arrhenius plot of Fig. 10. It appears that the activation energy for methanation is not a strong function of the hydrogen partial pressure. This is in agreement with the idea that CO dissociation is the rate-limiting step in CO methanation. However, at higher hydrogen pressure the rate of the reaction increases. This must be due to the creation of an increased number of active sites. High hydrogen pressures will result in a faster removal of the surface oxygen species remaining after CO dissociation. This results in a larger number of free rhodium surface sites, which can be used for CO dissociation. Some authors have indicated that the dissociation of CO (*46, 47*) and CO_2 (*48*) is enhanced by hydrogen. However, we note only an enhancement in the number of active sites, while the activation energy for CO methanation is independent of the hydrogen partial pressure.

TPSR can also be used to study the reactivity of surface species that are formed from CO decomposition at elevated temperatures. Figure 11 shows such a plot in which the hydrogenation activity of surface species created from CO adsorption at 400°C is shown. After CO adsorption at 400°C, the catalyst was quickly cooled in a helium flow to 50°C. During the adsorption of CO at 400°C a very reactive carbonaceous surface species that is hydrogenated towards methane at 50°C is formed. Even at −15°C methane formation was detected upon hydrogenation. This highly reactive carbon species

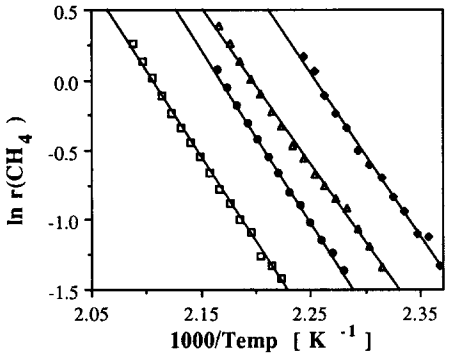

FIG. 10. Arrhenius plot from TPSR curves with different hydrogen partial pressures on the rhodium/Grace silica catalyst. Squares, P_{H_2} = 37 mbar; circles, P_{H_2} = 80 mbar; triangles, P_{H_2} = 160 mbar; diamonds, P_{H_2} = 440 mbar.

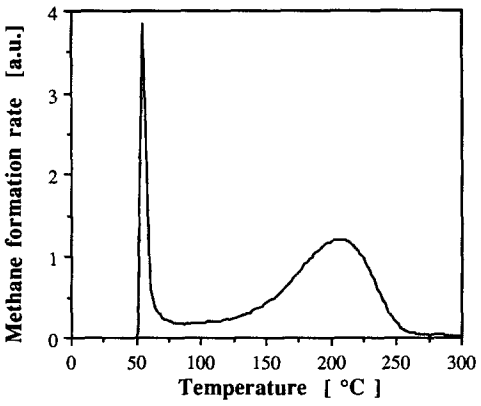

FIG. 11. TPSR of surface species remaining after CO adsorption at 400°C on the Rh/Grace silica catalyst.

is created by CO dissociation at temperatures above 250°C. It was first detected by Solymosi and Erdöhelyi (*15*) who indicated it as a carbidic type of carbon which can be transformed during "aging" into a less reactive graphitic phase.

The high hydrogenation rate of surface carbon is consistent with CO dissociation being the rate-limiting step in CO methanation. The second peak in the TPSR of Fig. 11 is at the temperature where nondissociated CO reacts. This peak can therefore be described to undissociated CO, which is still present on the catalyst surface. This was confirmed by additional FT/IR experiments in which adsorbed CO was still visible after a temperature treatment at 400°C.

Integrating the first and second peak from Fig. 11 it is possible to define a fraction reactive carbon to total hydrogenatable species. Formation of methane below 100°C is defined as due to reactive carbon; during TPSR of adsorbed CO below this temperature no methane is produced (Fig. 5). The influence of vanadium on the formation of reactive surface carbon was investigated at different CO adsorption temperatures (Fig. 12). The fraction of reactive carbon formed from CO is a function of the adsorption temperature. Its formation is an activated process. The fraction of reactive carbon produced from CO is increased by vanadium promotion and the temperature of initial formation is lowered by 50°C. This again indicates a faster CO dissociation rate on the vanadium-promoted catalyst. Reactive carbon can also be created from room temperature-adsorbed CO and subsequent heating of the catalyst. The fraction of reactive surface carbon formed in this way is less than that formed directly from CO adsorption from the gas phase. The effective activation energy for CO dissociation is less in the last case and equal to the activation energy for dissociation of the chemisorbed state minus the heat of CO adsorption (*49*).

It is of interest to study the incorporation of carbidic surface carbon generated by CO decomposition into products consisting of more than one carbon atom during a synthesis gas reaction. Efstathiou and Bennett (*50*) showed that the surface concentration of reactive C_α surface carbonaceous species can vary from 2 to 6% during synthesis gas reaction on an alumina-supported rhodium catalyst. We have seen that vanadium can increase this value due to an enhanced rate of CO dissociation (*56*). However, to compare intrinsic reactivity for carbon–carbon bond formation between these carbidic surface species, it is important that the surface coverages are the same on the two catalysts. This is made possible by choosing the right CO adsorption temperature from Fig. 12.

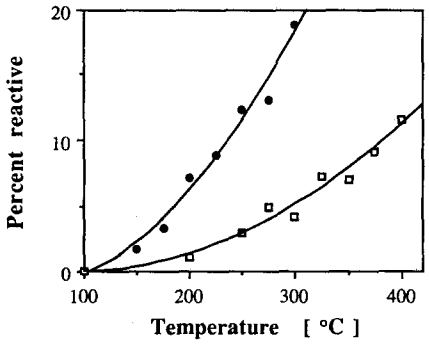

FIG. 12. Fraction of reactive carbon formed from CO as measured with TPSR, as a function of the CO adsorption temperature, for the Rh/Aerosil (squares) and the RhV/Aerosil (circles) catalyst.

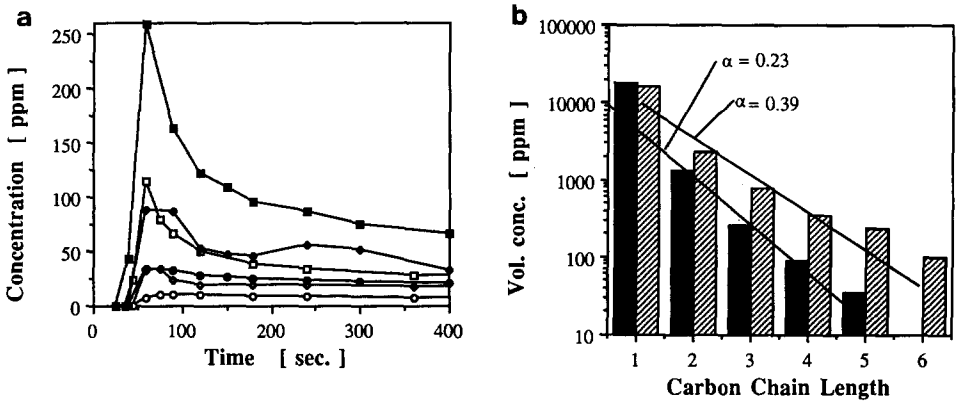

FIG. 13. (a) Propane (squares), butane (diamonds), and pentane (circles) formation during the start of a synthesis gas reaction at 200°C with (solid symbols) and without (open symbols) predeposition of surface carbon on Rh/Grace silica. (b) Hydrocarbon distribution after deposition of reactive carbon during the start of a synthesis gas reaction on rhodium/Grace silica (black bars) and rhodium–vanadium/Grace silica (lined bars).

Here we generated a surface coverage of about 14% on a Rh and a RhV catalyst. Subsequently the formation of higher hydrocarbons can be initiated by flowing a flow of 15 ml/min of $H_2/CO = 2$ at 200°C over the catalyst. The initial concentrations of hydrocarbons formed were measured by a time-based GC analysis (*51*). In Fig. 13 the incorporation of reactive surface carbon from CO into hydrocarbon is compared with hydrocarbon formation from synthesis gas without predeposition.

Methane to pentane product formation is higher after predeposition of surface carbon on the rhodium catalyst (Fig. 13a) and also on the rhodium–vanadium catalyst. This indicates that the reactive carbidic surface carbon is incorporated in a synthesis gas reaction and is therefore a reaction intermediate. This was also proven with labeled ^{13}CO on nickel by Araki and Ponec (*52*) and on cobalt and ruthenium by Biloen and coworkers (*53–55*). They deposited ^{13}C carbon from ^{13}CO decomposition, which could be incorporated into hydrocarbons in synthesis gas conditions.

The reactive C_α surface species especially show high affinity for C–C bond formation on rhodium catalysts (*51*). On the vanadium-promoted catalyst reactive surface carbon incorporates to a larger extent into higher hydrocarbons. Figure 13b shows an enhanced selectivity for carbon–carbon bond formation caused by vanadium. The chance for chain growth is increased by about 70%. Previously (*49, 51*) we ascribed this effect to an enhanced metal–carbon interaction on the vanadium-promoted catalyst.

CONCLUSION

Both TPSR and PSRA show that CO dissociation on rhodium catalysts is enhanced by vanadium promotion. This is due to a reduction of the apparent activation energy by about 27 kJ/mol. While the activation energy for CO dissociation is independent of the hydrogen partial pressure, it is a strong function of the CO surface concentration. From this dependence it is possible to estimate the optimum surface coverage for methanation. It is found to be weakly temperature dependent and of the order of 0.2–0.3.

The activation energy for CO dissociation depends strongly on the number of free sites. Therefore enhanced rates for CO dissociation in the presence of reduced vanadium patches can be due to the supply of a

new kind of oxygen vacancies, increasing the rate of CO dissociation.

Dissociative CO adsorption at temperatures above 250°C produces a very reactive carbidic surface species. Its formation is enhanced by coadsorption of vanadium. This carbon species can be incorporated into hydrocarbons in synthesis gas condition. Vanadium promotes the reactivity of this surface carbide to the formation of higher hydrocarbons.

ACKNOWLEDGMENTS

The Dutch organization for fundamental chemical research SON is acknowledged for its financial support. We thank Johnson and Matthey for the free use of their high-purity rhodium chemicals.

REFERENCES

1. Bhasin, M. M., and O'Conner, G. L., Belgian Patent 824,822 to Union Carbide Corp. (1975).
2. Ellgen, P. C., Bartley, W. J., Bhasin, M. M., and Wilson, T. P., *Adv. Chem.* **178,** 147 (1979).
3. Bhasin, M. M., Bartley, W. J., Ellgen, P. C., and Wilson, T. P., *J. Catal.* **54,** 120 (1978).
4. van den Berg, F. G. A., Glezer, J. H. E., and Sachtler, W. M. H., *J. Catal.* **93,** 340 (1985).
5. van der Lee, G., Bastein, A. G. T. M., van den Boogert, J., Sculler, B., Luo, H-Y., and Ponec, V., *J. Chem. Soc. Faraday Trans. 1* **83,** 2103 (1987).
6. Sachtler, W. M. H., and Ichikawa, M., *J. Phys. Chem.* **90,** 4752 (1986).
7. Mori, T., Miyamoto, M., Takahashi, N., Fukagaya, M., Niizuma, H., Hattori, T., and Murakami, Y., *J. Chem. Soc. Chem. Commun.*, 678 (1984).
8. Bond, G. C., and Richards, D. G., *Appl. Catal.* **28,** 303 (1986).
9. Underwood, R. P., and Bell, A. T., *Appl. Catal.* **21,** 157 (1986).
10. van der Lee, G., Schuller, B., Post, H., Favre, T. L. F., and Ponec, V., *J. Catal.* **98,** 522 (1986).
11. Bastein, A. G. T. M., Luo, H. Y., Mulder, A. A. J. P., and Ponec, V., *Appl. Catal.* **38,** 241 (1988).
12. Gorodetskii, V. V., and Nieuwenhuys, B., *Surf. Sci.* **105,** 299 (1981).
13. Castner, P., and Somorjai, G. A., *Surf. Sci.* **83,** 60 (1979).
14. Castner, P., and Somorjai, G. A., *Surf. Sci.* **103,** L134 (1981).
15. Solymosi, F., and Erdöhelyi, A., *Surf. Sci.* **110,** L630 (1981).
16. Katzer, J. R., Sleight, A. W., Gajardo, P., Michel, J. B., Gleason, E. F., and McMillan, S., *Faraday Discuss. Chem. Soc.* **72**(8), (1981).
17. Mochida, I., Ikeyama, N., Ishibashi, H., and Fulitsu, H., *J. Catal.* **110,** 159 (1988).
18. Gilhooley, K., Jackson, S. D., and Rigby, S., *Appl. Catal.* **21,** 349 (1986).
19. Erdöhelyi, A., and Solymosi, F., *J. Catal.* **84,** 446 (1983).
20. Ichikawa, M., Fukushima, T., and Shikakura, K., *in* "Proceedings, 8th International Congress on Catalyis, Berlin, 1984," Vol. 2, p. 69. Dechema, Frankfurt-am-Main, 1984.
21. de Koster, A., Jansen, A. P. J., Geerlings, J. J. C., and van Santen, R. A., *Faraday Discuss Chem. Soc.* **87,** 263 (1989).
22. Fujimoto, K., Kameyama, M., and Kung, T., *J. Catal.* **61,** 7 (1980).
23. Sachtler, W. M. H., Shriver, D. F., Hollenberg, W. B., and Lang, A. F., *J. Catal.* **92,** 429 (1985).
24. Lavalley, J. C., Saussey, J., Lamotte, J., Breault, R., Hindermann, J. P., and Kiennemann, A., *J. Phys. Chem.* **19**(15), 5941 (1990).
25. Stevenson, S. A., Lisifsin, A., and Knözinger, H., *J. Phys. Chem.* **94**(4), 1576 (1990).
26. Ichikawa, M., Hoffmann, P. E., and Fukuoka, A., *J. Chem. Soc. Chem. Commun.* **18,** 1395 (1989).
27. Fukuoka, A., Kimura, T., Rao, L-F., and Ichikawa, M., *Catal. Today* **6,** 55 (1989).
28. Ichikawa, M., and Fukushima, T., *J. Phys. Chem.* **89,** 1564 (1985).
29. Low, G. G., and Bell, A. T., *J. Catal.* **57,** 397 (1979).
30. McCarty, J. G., and Wise, H., *J. Catal.* **57,** 406 (1979).
31. Bastein, A. G. T. M., Ph.D. thesis, Leisden, 1988.
32. Mori, T., Miyamoto, M., Niizuma, H., Takahashi, N., Hattori, T., and Murakami, Y., *J. Phys. Chem.* **90,** 109 (1986).
33. Tauster, S. J., Fung, S. C., and Garten, R. L., *J. Am. Chem. Soc.* **100,** 170 (1978).
34. Kip, B. J., Smeets, P. A. T., van Wolput, J. H. M. C., Zandbergen, H., van Grondelle, J., and Prins, R., *Appl. Catal.* **33,** 157 (1987).
35. van den Berg, F. G. H., Ph.D. thesis, Leiden, 1983.
36. Vogt, E. C. T., De Boer, M., Van Dillen, A. J., and Geus, J. W., *Appl. Catal.* **40,** 255 (1988).
37. den Hartog, A. G., Deug, M., Jongerius, F., and Ponec, V., *J. Mol. Catal.*, in press.
38. Burton, J. J., *Catal. Rev. Sci. Eng.* **9,** 209 (1974).
39. Nonneman, L. E. Y., Bastein, A. G. T. M., Ponec, V., and Burch, R., *Appl. Catal.* **68,** L23 (1990).
40. Nonneman, L. E. Y., and Ponec, V., *Catal. Lett.* **7,** 197 (1990).
41. Mori, Y., Mori, T., Miyamoto, M., Hattori, T., and Murakami, Y., *Appl. Catal.* **66,** 59 (1990).
42. Taniguchi, S., Mori, T., Mori, Y., Miyamoto, M., Hattori, T., and Murakami, Y., *J. Catal.* **116,** 108 (1989).
43. Falconer, J. L., and Schwarz, J. A., *Catal. Rev. Sci. Eng.* **25**(2), 141 (1983).

44. de Jong, A. M., and Niemantsverdriet, J. W., *Surf. Sci.* **223,** 355 (1990).
45. Marbrow, R. A., and Lambert, R. M., *Surf. Sci.* **67,** 489 (1977).
46. Solymosi, F., Tombáckz, I., and Cocksis, M., *J. Catal.* **75,** 78 (1982).
47. Siddall, J. H., Miller, M. L., and Delgass, W. N., *Chem. Eng. Commun.* **83,** 261 (1989).
48. Henderson, M. A., and Worley, S. D., *J. Phys. Chem.* **89,** 1417 (1985).
49. van Santen, R. A., de Koster, A., and Koerts, T., *Catal. Lett.* **7,** 1 (1990).
50. Efstathiou, A. M., and Bennett, C. O., *J. Catal.* **120,** 118 (1989).
51. Koerts, T., and van Santen, R. A., *Catal. Lett.* **6,** 49 (1990).
52. Araki, M., and Ponec, V., *J. Catal.* **44,** 439 (1976).
53. Biloen, P., Helle, J. N., and Sachtler, W. M. H., *J. Catal.* **58,** 95 (1979).
54. Sachtler, W. M. H., Biloen, P., and Helle, J. N., *in* "Proceedings, International Conference Heterog. Catal., Varna, 1979."
55. Biloen, P., and Sachtler, W. M. H., *in* "Advances in Catalysis" (D. D. Eley, H. Pines, and P. B. Weisz, Eds.), Vol. 30, p. 165. Academic Press, San Diego, 1981.
56. Koerts, T., Welters, W. J. J., van Santen, R. A., Nonneman, L. E. Y., and Ponec, V., *in* "Natural Gas Conversion" (A. Holmen, K-J. Jens, and S. Kolboe, Eds.), Elsevier, Amsterdam, 1990.